

Stable and efficient quantum-dot light-emitting diodes based on solution-processed multilayer structures

Lei Qian[†], Ying Zheng[†], Jiangeng Xue^{*} and Paul H. Holloway^{*}

Multilayer, colloidal quantum-dot based light-emitting diodes that exhibit high brightness, solution processability, colour tunability and narrow emission bandwidth are reported. These devices consist of a quantum-dot emissive layer sandwiched between an organic hole transport layer and an electron transport layer of ZnO nanoparticles, all of which are deposited using a solution process. The devices have maximum luminance and power efficiency values of 4,200 cd m⁻² and 0.17 lm W⁻¹ for blue emission, 68,000 cd m⁻² and 8.2 lm W⁻¹ for green, and 31,000 cd m⁻² and 3.8 lm W⁻¹ for orange-red. Moreover, with the incorporation of the ZnO nanoparticles, these devices exhibit high environmental stability, and the unencapsulated devices have operating lifetimes exceeding 250 h in low vacuum with an initial brightness of 600 cd m⁻².

In the past decade, several research groups have demonstrated various lighting-emitting diodes (LEDs) using colloidal quantum dots (QDs) as the emitting layers^{1–5}. Interest in these devices stems from the efficient and narrow-band emissions from the QDs that can be easily tuned by varying the size of the QDs. The maximum brightness and current efficiency of such QD-LEDs have steadily increased from ~100 cd m⁻² and 0.2 cd A⁻¹ to ~10,000 cd m⁻² and 3 cd A⁻¹, respectively^{4,5}. Currently, an organic electron transport layer (ETL) composed of vacuum-deposited small molecules is widely used to balance charge transport and facilitate electron injection into QD emissive layers (EMLs). However, small-molecule ETLs suffer from a few drawbacks that could limit future commercialization. Compared with inorganic QD EMLs, the small-molecule charge transport layer has inferior thermal stability and is more susceptible to degradation induced by oxygen and/or moisture. Moreover, a combination of solution and vacuum deposition processes complicates the QD-LED fabrication process and reduces the throughput compared to all solution-based manufacturing techniques. Therefore, a solution-processable inorganic charge transport layer for a QD EML would be desirable for efficient and stable QD-LEDs that are more amenable to high-throughput manufacturing. Vacuum-deposited, amorphous metal-oxide charge transport layers for QD-LEDs have already been demonstrated by others, with a maximum brightness of 1,950 cd m⁻² and current efficiency of 0.064 cd A⁻¹ being achieved⁶. More recently, amorphous TiO₂ charge transport layers prepared by a sol-gel method have been introduced, resulting in all-solution-processed QD-LEDs with a maximum brightness of 12,380 cd m⁻² and efficiency of 2.5 cd A⁻¹ (ref. 5). However, amorphous metal oxides have relatively low carrier mobility compared with their crystalline phase. For instance, amorphous TiO₂ has an electron mobility of only ~1 × 10⁻⁴ cm² V⁻¹ s⁻¹, which is four orders of magnitude lower than that in crystalline TiO₂ (~1 cm² V⁻¹ s⁻¹)⁷. Moreover, hydrolysis through thermal annealing at 100 °C is needed to convert the sol-gel precursor into amorphous TiO₂.

In this study, we obtain bright, efficient QD-LEDs using a solution-processable crystalline ZnO nanoparticle layer as the ETL

in combination with a thermally polymerizable polymer as the hole transport layer (HTL). Such all-solution-processable QD-LEDs using ZnO nanoparticles demonstrate maximum brightness levels of 4,200 cd m⁻², 68,000 cd m⁻² and 31,000 cd m⁻² for emission of blue, green and orange-red light, respectively, which are the highest values of brightness reported to date. The ZnO nanoparticles ETL also required reduced driving voltage and demonstrated improved luminance power efficiency. The turn-on voltages (driving voltage corresponding to a luminance of 0.1 cd m⁻²) and peak power efficiencies were 2.4 V and 0.17 lm W⁻¹ for blue, 1.8 V and 8.2 lm W⁻¹ for green, and 1.7 V and 3.8 lm W⁻¹ for orange-red emitting devices, respectively. In addition, continuous operation of ZnO nanoparticle-based QD-LEDs in low vacuum yielded a lifetime of 270 h with an initial luminance of 600 cd m⁻².

The ZnO nanoparticles used in the current study were synthesized with a solution-precipitation method⁸, the details of which are provided in the Methods. A transmission electron microscope (TEM) image of the ZnO nanoparticles is shown in Fig. 1a, indicating that the ZnO nanoparticles have an average diameter of ~3 nm. Lattice fringes can be clearly observed in the high-resolution TEM image shown in the inset, which suggests good crystallinity of the ZnO nanoparticles. The X-ray diffraction pattern (XRD) of the ZnO nanoparticles together with that of bulk phase ZnO are shown in Fig. 1b. Comparison of the diffraction peaks suggests that the ZnO nanoparticles are crystalline and adopt a wurtzite structure similar to that of bulk ZnO. The small particle size leads to a significant broadening of the characteristic diffraction peaks from the ZnO nanoparticles.

The structure of the ZnO nanoparticle-based QD-LEDs is schematically shown in Fig. 1c, with the devices consisting of layers of indium tin oxide (ITO)/poly(ethylenedioxythiophene):polystyrene sulphonate (PEDOT:PSS) (40 nm)/poly(*N,N'*-bis(4-butylphenyl)-*N,N'*-bis(phenyl)benzidine) (poly-TPD) (45 nm)/CdSe-ZnS core-shell QDs (13–25 nm)/ZnO nanoparticles (25–75 nm)/Al. With the exception of the Al cathode, which was deposited using vacuum thermal evaporation, all other layers were sequentially deposited on ITO by spin-coating. Achieving the multilayer

Department of Materials Science and Engineering, University of Florida, Gainesville, Florida 32611-6400, USA; [†]These authors contributed equally to this work. *e-mail: jxue@mse.ufl.edu; pholl@mse.ufl.edu

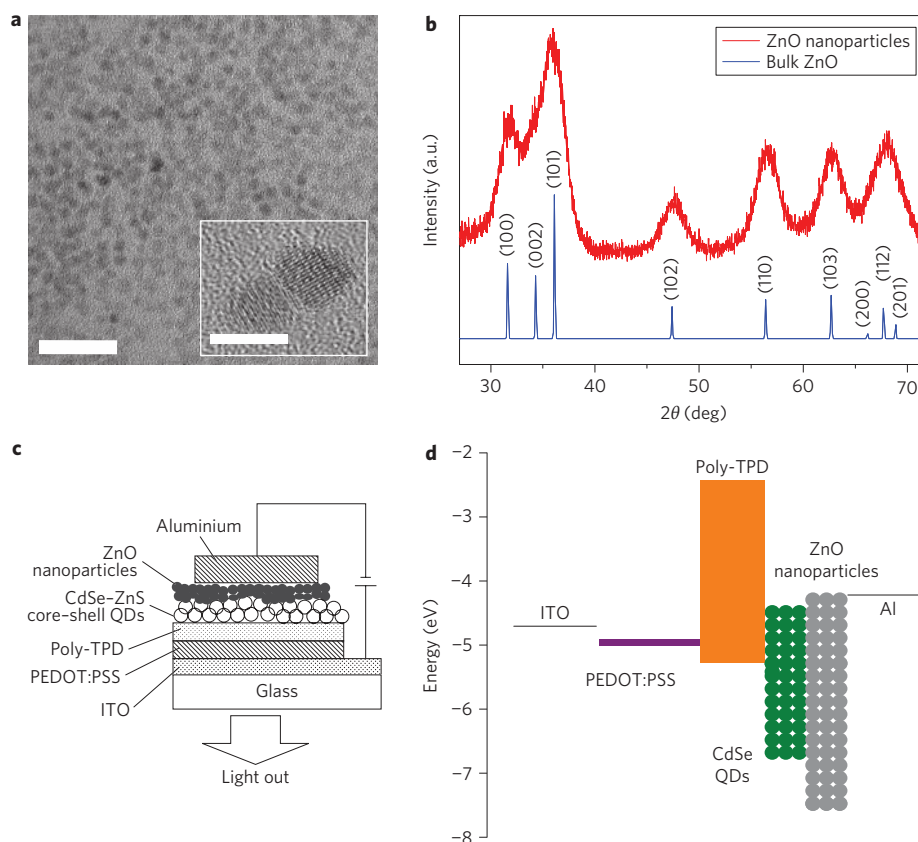


Figure 1 | Crystallinity and XRD data, schematic of layered device, and energy levels of the ZnO nanoparticle-based QD-LED. **a**, TEM image of ZnO nanoparticles (scale bar, 20 nm). Inset: High-resolution TEM images of same ZnO nanoparticles showing lattice fringes (scale bar, 3 nm). **b**, XRD pattern from ZnO nanoparticles (red) together with that from bulk wurtzite ZnO (blue). **c**, Schematic of layers in the device structure. **d**, Energy level diagram for the various layers.

structure using a solution process requires the use of orthogonal solvents to avoid compromising the integrity of the underlying layers while depositing overlayers. To this end, we used water, chlorobenzene, toluene and ethanol as the solvents for PEDOT:PSS, poly-TPD, CdSe-ZnS QDs and ZnO nanoparticles, respectively. As poly-TPD has been shown to resist nonpolar solvents such as toluene after annealing¹¹, these multilayer QD-LEDs can be potentially fabricated by high-throughput solution-processing techniques, such as inkjet printing^{2,9}. According to the schematic energy level diagram shown in Fig. 1d, with an electron affinity of ~ 4.3 eV and an ionization potential of ~ 7.6 eV (refs 10,11) the ZnO nanoparticle layer not only provides efficient electron injection from the Al cathode into CdSe-ZnS QDs, but also helps to confine holes within the QD layer due to the valence band offset at the QD/ZnO nanoparticle interface, leading to an improved charge recombination efficiency.

Figure 2a shows the current-density/luminance/voltage (J - L - V) characteristics of ZnO nanoparticle-based QD-LEDs with different light-emitting QDs in the EML. The maximum luminance for the blue, green and orange-red devices was 4,200, 68,000 and 31,000 cd m^{-2} , respectively. These values are a factor of 3–7 higher than previously reported highest luminances from QD-LEDs^{4,12}. These devices also exhibit rather low turn-on voltages of 2.4 V (blue), 1.8 V (green) and 1.7 V (orange-red), which are lower than the photon voltages of the corresponding devices (defined as the photon energy $h\nu$ divided by the electron charge e) because the peak emission wavelengths are $\lambda = 470$ nm ($h\nu = 2.6$ eV), 540 nm ($h\nu = 2.3$ eV) and 600 nm ($h\nu = 2.1$ eV) for blue, green and orange-red QD-LEDs, respectively. Electroluminescence spectra measured using a high-sensitivity spectrometer indicated that light

emission from the blue QD-LEDs was achieved at a driving voltage as low as 2.0 V (Supplementary Fig. S1), suggesting that electrons and holes can be efficiently injected into the QD EML at low driving voltages with the ZnO nanoparticle ETL. Holes and electrons are likely to accumulate at the interface between poly-TPD and the QD EML due to the large energy offset at this type II heterojunction. With opposite charges accumulating at the interface, an Auger-assisted hole injection process can take place, in which one high-energy hole can be obtained after absorbing the energy released from the interfacial recombination of an electron–hole pair. The resulting high-energy hole can overcome the injection barrier and recombine with an electron inside the QDs EML to emit a photon. Such an Auger-assisted energy upconversion model has been used to explain sub-gap electroluminescence observed from a number of organic–organic and organic–inorganic type II heterojunctions^{8,13}.

Voltages for the operation of these ZnO nanoparticle-based QD-LEDs at typical display and lighting brightness levels are also drastically lower than previously reported for QD-LEDs that use small-molecular ETLs^{1,2,4}. For example, the green emitting ZnO nanoparticle-based QD-LED reaches 100 cd m^{-2} and 1,000 cd m^{-2} at $V = 2.4$ V and 2.8 V, respectively, whereas QD-LEDs using tris(8-hydroxyquinoline) aluminium (Alq_3) as the ETL require 10.8 V and 13.5 V, respectively (Supplementary Fig. S2)⁵. Reduced driving voltages for the QD-LED are expected to lead to higher power efficiency and better device stability. We hypothesize that the Auger-assisted charge injection, which strongly depends on the level of electron injection into the QD layer, is the main reason for achieving such lower operating voltages. Devices with ZnO nanoparticles as the ETL showed significantly higher current density than devices without an ETL, or with an Alq_3 ETL (Supplementary Fig. S3). As the same

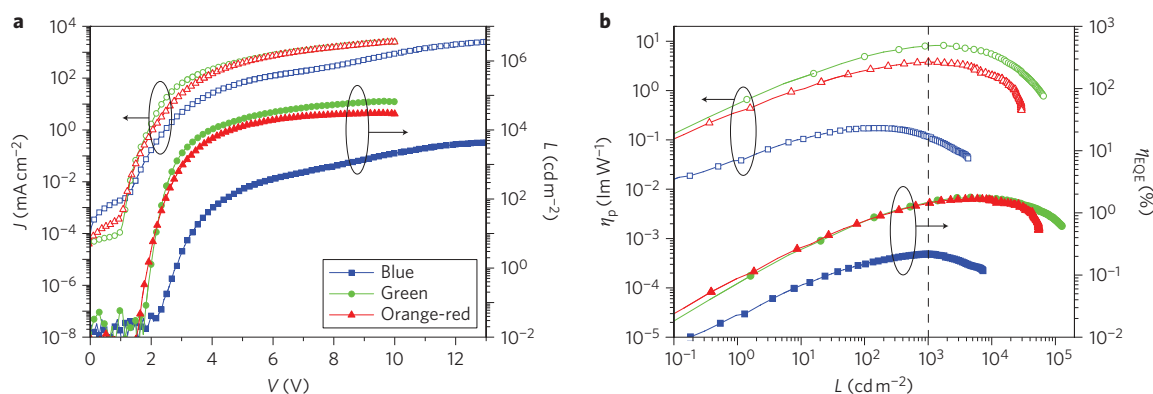


Figure 2 | Electroluminescence performance of ZnO nanoparticle-based QD-LEDs with blue, green and orange-red emission. a, Current-density (J) and luminance (L) versus driving voltage (V). **b,** Luminance power efficiency (η_p) and external quantum efficiency η_{EQE} versus luminance.

Table 1 | Comparison of turn-on voltage V_T , emission peak wavelength λ_{max} , FWHM, maximum luminance L_{max} , external quantum efficiency η_{EQE} , power efficiency η_p and luminous efficiency η_A of the three ZnO nanoparticle-based QD-LEDs.

Colour of QD-LED	V_T (V)	λ_{max} (nm)	FWHM (nm)	L_{max} (cd m ⁻²)	η_{EQE} (%)		η_p (lm W ⁻¹)		η_A (cd A ⁻¹)	
					Peak	@ 1,000 cd m ⁻²	Peak	@ 1,000 cd m ⁻²	Peak	@ 1,000 cd m ⁻²
Blue	2.4	470	28	4,200	0.22	0.21	0.17	0.12	0.32	0.31
Green	1.8	540	38	68,000	1.8	1.6	8.2	8.1	7.5	7.1
Orange-red	1.7	600	39	31,000	1.7	1.5	3.8	3.8	3.9	3.6

HTLs are used in these devices, the high current density in ZnO nanoparticle-based devices is attributed to the very efficient electron injection into the QD layer. With more electrons accumulated at the poly-TPD/QD interface, the interfacial recombination rate is much higher in the ZnO nanoparticle-based device than in other devices, which also suggests that the Auger process is efficient. Although the same Auger-assisted charge injection process can also take place at the poly-TPD/QD interface in Al-only or Alq₃/Al devices, the voltages required to build up a sufficient concentration of electrons for an efficient Auger process at the poly-TPD/QD interface are much higher, presumably due to poor electron injection and/or transport. Thus, Al-only or Alq₃/Al devices do not exhibit a low-voltage turn-on from Auger-assisted charge injection. In contrast, electrons can be efficiently injected into a ZnO nanoparticle-based device even at low voltages of ~ 1 – 2 V (Supplementary Fig. S3) by the Auger process. The efficient electron injection is attributed to the higher electron mobility of ZnO nanoparticles as well as proper band alignments. The electron mobility of our crystalline ZnO nanoparticles was measured to be 2×10^{-3} cm² V⁻¹ s⁻¹ (Supplementary Fig. S4), which is lower than a previous report of 0.07 cm² V⁻¹ s⁻¹ (ref. 14), probably due to different ZnO nanoparticle size and processing conditions. However, our electron mobility is at least one order of magnitude higher than that of organic ETLs (typically $\sim 1 \times 10^{-4}$ cm² V⁻¹ s⁻¹ or lower)^{9,15}. In addition, the conduction band of ZnO is aligned with the Fermi level of Al and the conduction band of the green QDs (although the energy levels of the QDs do vary with size due to the quantum confinement effect), and apparently results in low energy barriers for electron injection from the cathode into the EML. All of the above factors result in the very low turn-on and operating voltages of the devices described here.

The luminance power η_p and external quantum efficiency η_{EQE} as a function of the luminance of the devices are shown in Fig. 2b. The ZnO nanoparticle-based QD-LEDs display maximum η_p and η_{EQE} values of 0.17 lm W⁻¹ and 0.22% , 8.2 lm W⁻¹ and 1.8% , and 3.8 lm W⁻¹ and 1.7% for blue, green and orange-red emission, respectively. Note that the peak efficiencies of the current QD-LEDs are achieved at high brightness (in the range 1×10^2 to 1×10^4 cd m⁻²), which are

more desired for practical display and lighting applications. At $1,000$ cd m⁻², the power efficiencies are $\eta_p = 0.12$, 8.1 and 3.8 lm W⁻¹ for blue, green and orange-red devices, respectively, and the corresponding luminous efficiencies are 0.31 , 7.1 and 3.6 cd A⁻¹. Table 1 summarizes the detailed performance parameters of the three different-coloured QD-LEDs of the present study.

It is noted that the device performance show a strong dependence on the thickness of the QD and ZnO nanoparticle layer. Figure 3 presents the turn-on voltage V_T and peak external quantum efficiency $\eta_{EQE,m}$ as a function of the QD and ZnO nanoparticle layer thickness for the green QD-LEDs. In Fig. 3a, with the QD layer fixed at 25 nm, the turn-on voltage of the device increases from 2.1 V to 3.4 V when the ZnO layer thickness is increased from 25 nm to 75 nm. However, the maximum $\eta_{EQE,m}$ of 1.4% is achieved with 35 -nm-thick ZnO, with a thicker ZnO layer inducing a fast roll-off of the efficiency. For a 35 nm ZnO layer, increasing the QD layer thickness from 13 to 25 nm resulted in a steady increase of both V_T and $\eta_{EQE,m}$ (Fig. 3b), but was much more dramatic for $\eta_{EQE,m}$. With the CdSe–ZnS QDs being ~ 6 nm in diameter, this suggests that multiple monolayers of QDs are needed for efficient recombination of electrons and holes to form excitons directly in the QD EML. This is very different from the earlier observation that only a monolayer of QD is needed, with the suggestion that excitons were formed elsewhere in the charge transport materials followed by energy transfer to the QDs^{1,16}. Moreover, Fig. 3b suggests that an even higher η_{EQE} could potentially be achieved with thicker QD layers. However, the thickness of the QD layer in our device is limited by the low concentration of the QD solution, because a slow spin speed of 500 r.p.m. has already been used to achieve the thickest QD layer. Nevertheless, the gain in η_{EQE} will eventually be offset by increased driving voltages for thicker QD layers, resulting in low power efficiencies. Further systematic optimization of both the QD and ZnO nanoparticle layer thickness is desired to realize better device performance.

The normalized electroluminescence spectra of the ZnO nanoparticle-based QD-LEDs at an operation voltage of 3 V are shown in Fig. 4a. The full-width at half-maximum (FWHM) is 28 nm, 38 nm and 39 nm for the blue, green and orange-red devices, respectively.

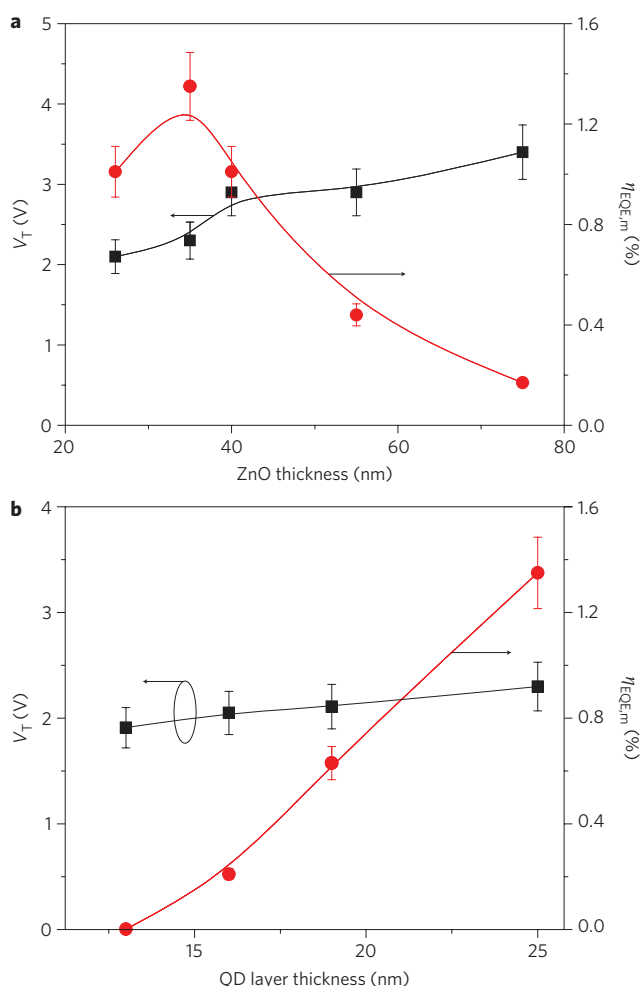


Figure 3 | Dependence of QD-LED performance on ZnO and QD layer thickness. **a**, Turn-on voltage (V_T) and maximum external quantum efficiency ($\eta_{EQE,m}$) versus ZnO nanoparticle layer thickness (QD layer thickness, 25 nm). **b**, V_T and $\eta_{EQE,m}$ versus QD layer thickness (ZnO nanoparticle layer thickness, 35 nm). Error bars represent variation about the average for 16 pixels on four devices, and is typically less than $\pm 10\%$.

The inset shows photographs of the three operating devices fabricated on 1 inch² substrates. All devices display nearly saturated colours that, as shown by the Commission Internationale de Eclairage (CIE) chromaticity diagram in Fig. 4b, lie outside but near the National Television System Committee (NTSC) standard colour triangle.

The luminance and driving voltage versus time for an unencapsulated green QD-LED in low vacuum (~ 0.1 torr) operated at a constant current of ~ 20 mA cm⁻² are shown in Fig. 5. The luminance was $L = 100$ cd m⁻² initially, but increased to $L = 600$ cd m⁻² within 2 h, after which it slowly decreased with operation time, reaching 300 cd m⁻² after 270 h. The driving voltage of the device increased from 2.8 V to 4.1 V over the 270 h testing period. In conventional QD-LEDs, LiF (or a low-workfunction metal such as Ca or Mg) is used in combination with Al contacts for an improved electron injection layer^{1,5,17}. However, these devices can be unstable due to air and moisture sensitivity of the cathode materials¹⁸. In contrast, the current ZnO nanoparticle-based QD-LEDs show drastically improved stability. In addition to being a stable oxide, the 35-nm-thick ZnO nanoparticles ETL could also serve as a barrier against diffusion of oxygen and water into the active layers.

The mechanism leading to the dramatic increase in the brightness and power efficiency of the QD-LEDs over the first 2 h of operation is attributed to passivation of surface trap states on the CdSe/ZnS QDs

by adsorbed oxygen and water. As discussed in ref. 19 and references therein, the luminance of CdSe–ZnS core–shell quantum dots becomes larger by factors ranging from 10% to 8,000% in matters of minutes to hours upon exposure to water vapour or moist oxygen^{19–21}. The time constant and factor for the increased luminance are reported to be functions of the experimental conditions, but the increase by 600% in 2 h for our QD-LEDs is well within reported values for similar QDs. As shown in Supplementary Fig. S5, the formation of carbonate compounds was detected by X-ray photoelectron spectroscopy (XPS) on the surface of unactivated QDs stored simply in humid laboratory air for five days. Activation of the CdSe–ZnS QD layer with photons, similar to the report in ref. 19, caused the formation of both carbonate and sulphate compounds on the QD surfaces after less than 3 h in humid laboratory air. Others have reported increased luminance and the formation of sulphates on CdS–ZnS core–shell nanoparticles following UV irradiation in humid air²². The formation of sulphate (but not carbonate) compounds on the CdSe–ZnS QD surfaces has been predicted¹⁹, but they could not be detected using XPS due to the formation of an adventitious silicon layer. In the same study¹⁹, following

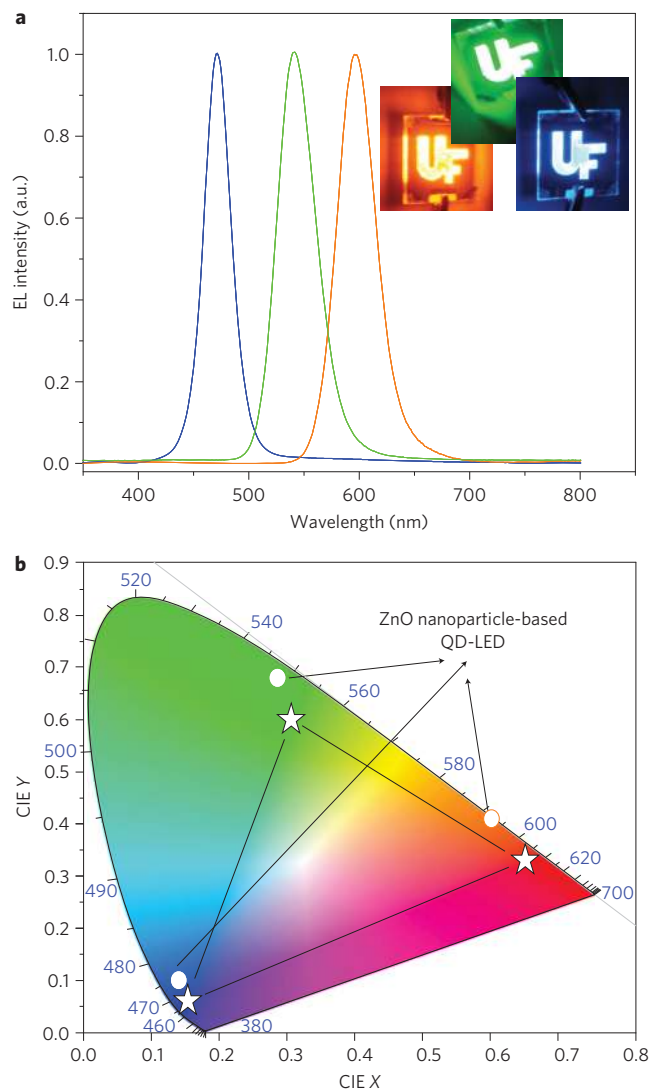


Figure 4 | Electroluminescence spectra and CIE coordinates of the QD-LEDs. **a**, Normalized electroluminescence spectra and images of QD-LEDs with peak emission wavelengths of 470 nm (blue), 540 nm (green) and 600 nm (orange-red). **b**, CIE coordinates of the three devices (circles) together with the NTSC colour standards (stars).

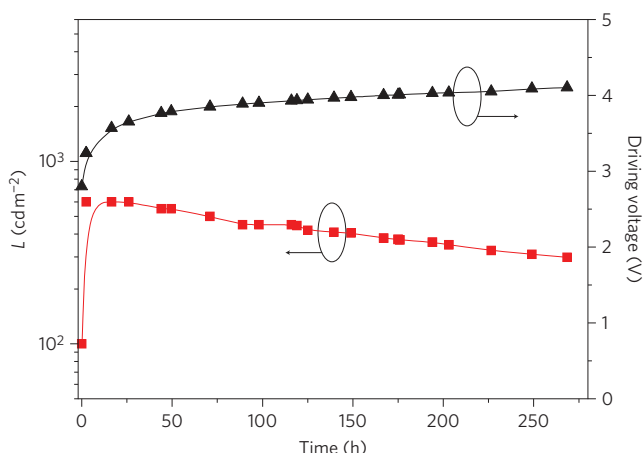


Figure 5 | Stability data for an unencapsulated green-emitting ZnO nanoparticle-based QD-LED. Luminance and driving voltage for a green emitting ZnO nanoparticle-based QD-LED versus time of operation in low vacuum (~ 0.1 torr) at room temperature with a constant driving current density of 20 mA cm^{-2} .

the rapid rise in photoluminescence brightness upon irradiation in moist oxygen, a decreased brightness was reported in periods of 0.25 h to a few hours¹⁹. In the present study, the ZnO nanoparticle layer stabilized the increased brightness and maintained it for periods of more than 250 h.

In summary, we have demonstrated very bright and very efficient, solution-processed QD LEDs using a ZnO nanoparticle ETL. The simple multilayer structure between the two electrodes, consisting of a conducting polymer hole injection layer, a conjugated polymer hole transport layer, a core-shell QD emissive layer and a ZnO nanoparticle electron transport layer, was entirely deposited using spin-coating from solutions with orthogonal solvents. The devices display maximum luminance and power efficiency values of $4,200 \text{ cd m}^{-2}$ and 0.17 lm W^{-1} , $68,000 \text{ cd m}^{-2}$ and 8.2 lm W^{-1} , and $31,000 \text{ cd m}^{-2}$ and 3.8 lm W^{-1} for blue, green and orange-red emissions, respectively. The device drive voltages at 600 cd m^{-2} were typically $\sim 4 \text{ V}$, and these low values were attributed to an Auger upconversion mechanism. Finally, unencapsulated device lifetimes of 270 h in low vacuum (~ 0.1 torr) at an initial luminance of 600 cd m^{-2} have been achieved.

Methods

Synthesis of CdSe-ZnS and ZnO nanoparticles. Orange-red, green and blue emitting CdSe-ZnS QDs with chemical-composition gradients were prepared according to a method reported in the literature²³. For a typical synthesis, 0.1 mmol of CdO, 4 mmol of zinc acetate and 5 ml of oleic acid were placed in a 50 ml flask and heated to 150°C in flowing high-purity N_2 for 30 min. Then 15 ml of 1-octadecene was added to the flask and the temperature increased to 300°C . A stock solution containing 2 ml of triethylphosphine, 0.2 mmol of Se and 3 mmol of S was quickly injected into the flask. The reaction temperature was maintained for 10 min and then cooled to room temperature. The resulting QDs were washed several times (minimum of three times) and finally dispersed in toluene at 10 mg ml^{-1} .

ZnO nanoparticles were synthesized by a solution-precipitation process using Zn acetate and tetramethylammonium hydroxide (TMAH)¹². For a typical synthesis, a solution of zinc acetate in dimethyl sulphoxide (DMSO) (0.5 M) and 30 ml of a solution of TMAH in ethanol (0.55 M) were mixed and stirred for 1 h in ambient air, then washed and dispersed in ethanol at a concentration of $\sim 30 \text{ mg ml}^{-1}$.

Fabrication and characterization of ZnO nanoparticle-based QD-LED. QD-LEDs were fabricated on glass substrates coated with ITO with a sheet resistance of $\sim 20 \Omega \text{ sq}^{-1}$. The substrates were cleaned with deionized water, acetone and isopropanol, consecutively, for 15 min each, and then treated for 15 min with ozone generated by ultraviolet light in air. These substrates were spin-coated with PEDOT:PSS (AI 4803) and baked at 150°C for 15 min in air. The coated substrates were then transferred to a N_2 -filled glove box for spin-coating of the poly-TPD, CdSe-ZnS QD and ZnO nanoparticle layers. Poly-TPD was purchased from American Dye Source and used for QD-LED devices without further purification.

The poly-TPD hole-transport layer was spin-coated using 1.5 wt% in chlorobenzene (2,000 r.p.m. for 30 s), followed by baking at 110°C for 30 min. This was followed by spin-coating of CdSe-ZnS QDs (10 mg ml^{-1} , toluene) and ZnO nanoparticles (30 mg ml^{-1} , ethanol) layers followed by baking at 145°C for 30 min. The spin speed varied from 500 to 2,000 r.p.m. for the QD layer and from 2,000 to 6,000 r.p.m. for the ZnO nanoparticle layer to achieve different layer thickness. These multilayer samples were then loaded into a custom high-vacuum deposition chamber (background pressure, $\sim 3 \times 10^{-7}$ torr) to deposit the top Al cathode (100 nm thick) patterned by an *in situ* shadow mask to form an active device area of 4 mm^2 . Current-luminance-voltage characteristics were measured using an Agilent 4155C semiconductor parameter analyser with a calibrated Newport silicon diode. The luminance was calibrated using a Minolta luminance meter (LS-100) according to the suggested method²⁴. The electroluminescence spectra were obtained with a JASCO FP750 spectrometer and a Keithley 2400 power source. Unless otherwise specified, all devices were stored and tested in air without any encapsulation. The continuous operation lifetime data shown in Fig. 5 are from devices tested in low vacuum (~ 0.1 torr).

Received 11 May 2011; accepted 29 June 2011;
published online 7 August 2011

References

- Anikeeva, P. O., Halpert, J. E., Bawendi, M. G. & Bulovic, V. Electroluminescence from a mixed red-green-blue colloidal quantum dot monolayer. *Nano Lett.* **7**, 2196–2200 (2007).
- Cho, K. S. *et al.* High-performance crosslinked colloidal quantum-dot light-emitting diodes. *Nature Photon.* **3**, 341–345 (2009).
- Coe, S., Woo, W. K., Bawendi, M. & Bulovic, V. Electroluminescence from single monolayers of nanocrystals in molecular organic devices. *Nature* **420**, 800–803 (2002).
- Colvin, V. L., Schlamp, M. C. & Alivisatos, A. P. Light-emitting-diodes made from cadmium selenide nanocrystals and a semiconducting polymer. *Nature* **370**, 354–357 (1994).
- Sun, Q. *et al.* Bright, multicoloured light-emitting diodes based on quantum dots. *Nature Photon.* **1**, 717–722 (2007).
- Caruge, J. M., Halpert, J. E., Wood, V., Bulovic, V. & Bawendi, M. G. Colloidal quantum-dot light-emitting diodes with metal-oxide charge transport layers. *Nature Photon.* **2**, 247–250 (2008).
- Feng, X. J. *et al.* Vertically aligned single crystal TiO_2 nanowire arrays grown directly on transparent conducting oxide coated glass: synthesis details and applications. *Nano Lett.* **8**, 3781–3786 (2008).
- Qian, L. *et al.* Electroluminescence in light emitting polymers at sub-bandgap voltages. *Nano Today* **5**, 384–389 (2010).
- Forrest, S. R. The path to ubiquitous and low-cost organic electronic appliances on plastic. *Nature* **428**, 911–918 (2004).
- Beek, W. J. E., Wienk, M. M. & Janssen, R. A. J. Efficient hybrid solar cells from zinc oxide nanoparticles and a conjugated polymer. *Adv. Mater.* **16**, 1009–1013 (2004).
- Ravirajan, P. *et al.* Hybrid polymer/zinc oxide photovoltaic devices with vertically oriented ZnO nanorods and an amphiphilic molecular interface layer. *J. Phys. Chem. B* **110**, 7635–7639 (2006).
- Tan, Z. N. *et al.* Bright and color-saturated emission from blue light-emitting diodes based on solution-processed colloidal nanocrystal quantum dots. *Nano Lett.* **7**, 3803–3807 (2007).
- Pandey, A. K. & Nunzi, J. M. Rubrene/fullerene heterostructures with a half-gap electroluminescence threshold and large photovoltage. *Adv. Mater.* **19**, 3613–3617 (2007).
- Roest, A. L., Kelly, J. J., Vanmaekelbergh, D. & Meulenkaamp, E. A. Staircase in the electron mobility of a ZnO quantum dot assembly due to shell filling. *Phys. Rev. Lett.* **89**, 036801 (2002).
- Eom, S. H. *et al.* Effect of electron injection and transport materials on efficiency of deep-blue phosphorescent organic light-emitting devices. *Org. Electron.* **10**, 686–691 (2009).
- Coe-Sullivan, S., Steckel, J. S., Woo, W. K., Bawendi, M. G. & Bulovic, V. Large-area ordered quantum-dot monolayers via phase separation during spin-casting. *Adv. Funct. Mater.* **15**, 1117–1124 (2005).
- Bae, W. K. *et al.* Highly efficient green-light-emitting diodes based on CdSe@ZnS quantum dots with a chemical-composition gradient. *Adv. Mater.* **21**, 1690–1694 (2009).
- Aziz, H. *et al.* Degradation processes at the cathode/organic interface in organic light emitting devices with Mg:Ag cathodes. *Appl. Phys. Lett.* **72**, 2642–2644 (1998).
- Pechstedt, K., Whittle, T., Baumberg, J. & Melvin, T. Photoluminescence of colloidal CdSe/ZnS quantum dots: the critical effect of water molecules. *J. Phys. Chem. C* **114**, 12069–12077 (2010).
- Cordero, S. R., Carson, P. J., Estabrook, R. A., Strouse, G. F. & Buratto, S. K. Photo-activated luminescence of CdSe quantum dot monolayers. *J. Phys. Chem. B* **104**, 12137–12142 (2000).
- Dembski, S. *et al.* Photoactivation of CdSe/ZnS quantum dots embedded in silica colloids. *Small* **4**, 1516–1526 (2008).

22. Yang, H. & Holloway, P. H. Efficient and photostable ZnS-passivated CdS:Mn luminescent nanocrystals. *Adv. Funct. Mater.* **14**, 152–156 (2004).
23. Bae, W. K., Char, K., Hur, H. & Lee, S. Single-step synthesis of quantum dots with chemical composition gradients. *Chem. Mater.* **20**, 531–539 (2008).
24. Forrest, S. R., Bradley, D. D. C. & Thompson, M. E. Measuring the efficiency of organic light-emitting devices. *Adv. Mater.* **15**, 1043–1048 (2003).

Acknowledgements

L.Q. and P.H.H. were supported by the Army Research Office (grant no. W911NF-07-1-0545). Y.Z. and J.X. were partially supported by the US Department of Energy (grant no. DE-FG36-08GO18020) and the Florida Energy Systems Consortium. Assistance in data collection and reduction by E. Lambers and K. Siebein of the Major Analytical Instrumentation Center at the University of Florida is gratefully acknowledged.

Author contributions

L.Q. and Y.Z. synthesized material, fabricated devices, collected performance data and postulated mechanisms to explain the excellent performance of the QD-LEDs. J.X. and P.H.H. supervised the synthesis of material and devices, directed the collection and reduction of performance data, designed tests for the postulated mechanisms, and finalized the manuscript.

Additional information

The authors declare no competing financial interests. Supplementary information accompanies this paper at www.nature.com/naturephotonics. Reprints and permission information is available online at <http://www.nature.com/reprints>. Correspondence and requests for materials should be addressed to J.X. and P.H.H.